Rare Metal Materials and Engineering
Volume 48, Issue 12, December 2019
Available online at www.rmme.ac.cn

Science Press

Cite this article as: Rare Metal Materials and Engineering, 2019, 48(12): 3812-3818.

ARTICLE

Effect of Aging Temperature on Microstructural Evolution and Mechanical Properties of a Novel *β* Titanium Alloy

Zhang Haoyu[1,2], Li Xiaohui[1], Lin Li[2], Zhang Siqian[2], Wang Chuan[3], Chen Lijia[2]

[1] Guangdong Provincial Key Laboratory for Technology and Application of Metal Toughening, Guangzhou 510650, China; [2] Shenyang University of Technology, Shenyang 110870, China; [3] Shenyang Aerospace Xinguang Group Co., Ltd, Shenyang 110861, China

Abstract: A *β* titanium alloy Ti-6Mo-5V-3Al-2Fe (wt%) was designed in terms of *d*-electron alloy design method. Aging treatment was performed at various temperatures ranging from 450 °C to 600 °C for 4 h to study the effect of aging temperature on microstructure evolution and tensile properties. The results show that the secondary *α* phase with smaller size and inter-particle spacing forms under *ω*-assisted nucleation mechanism at the aging temperature of 500 °C. The highest ultimate tensile strength of 1510 MPa is obtained due to the strengthening of fine acicular secondary *α* phases within *β* grains, while poor elongation of 4.6% is found as a result of the inevitable precipitation of *α* phase at grain boundaries and the formation of precipitate free zone near grain boundaries. Fine secondary *α* precipitates tend to coarsen with increasing the aging temperature. Coarse *α* precipitates can bring about broad inter-particle spacing and result in less *α*/*β* interfaces that act as effective dislocation barriers. The increase of aging temperature leads to the variation of tensile properties, i.e. the strength decreases while ductility changes in an opposite way. A considerable improvement of elongation to 12.2% is achieved by increasing the aging temperature to 600 °C, in association with the formation of parallel *α* colony near *β* grain boundaries and broad inter-particle spacing of secondary *α* phases within *β* grains.

Key words: *β* titanium alloy; aging; secondary *α* phase; microstructure; mechanical properties

β titanium alloys have attracted much attention due to their high strength-to-weight ratio, corrosion resistance and good formability[1,2]. Particularly, the *β* titanium alloys have been widely used in the aerospace industries because of their optimal combination of strength and toughness[3,4]. For example, the Ti-5Al-5Mo-5V-1Cr-1Fe (Ti-55511) alloy and the Ti-10V-2Fe-3Al (Ti-1023) alloy have been applied to the landing gear forgings of Airbus-350 and Boeing 777, respectively[5,6]. It is well known that the characteristics of phases in *β* titanium alloy, such as the stability, morphology, size and distribution, play important roles in the mechanical properties[7-9]. Meanwhile, lots of literatures indicated that the microstructure is strongly affected by processing parameters during aging treatment[10,11]. In fact, for *β* titanium alloys with different alloy composition, rules of microstructure evolution during aging treatment are different, resulting in different change rules of mechanical properties. For Ti-3Al-5Mo-6V-3Cr-2Sn-0.5Fe alloy, secondary *α* phase with the highest volume fraction and the smallest size is precipitated and meanwhile the highest yield strength can be obtained at a relatively low aging temperature of 440 °C [12]. Ti-8V-1.5Mo-2Fe-3Al alloy, which was modified from commercial Ti-1023 alloy, has well balanced combination of strength and ductility when aged at 550~600 °C[13]. Thus, it is still necessary to investigate the influence of aging treatment on the microstructure so as to improve the mechanical properties.

Ti-6Mo-5V-3Al-2Fe (wt%) alloy (referred to as Ti-6532) was newly designed according to the *d*-electron alloy design method. The *d*-electron alloy design method was developed by Abdel-Hady based on the cluster DV-Xα method[14]. Previously this method has been specifically used for the design and optimization of elastic properties[15]. In recent studies, this

Received date: December 19, 2018
Foundation item: Foundation of Guangdong Provincial Key Laboratory for Technology and Application of Metal Toughening (GKL201608); Foundation of Liaoning Province Educational Committee (LGD2016019)
Corresponding author: Zhang Haoyu, Ph. D., Lecturer, School of Materials Science and Engineering, Shenyang University of Technology, Shenyang 110870, P. R. China, Tel: 0086-24-25494501, E-mail: zhanghaoyu@sut.edu.cn

Copyright © 2019, Northwest Institute for Nonferrous Metal Research. Published by Science Press. All rights reserved.

method has been employed to design new titanium alloys exhibiting specific deformation mechanism and phase stability[16]. In the present work, based on commercial Ti-1023 alloy, Ti-6532 alloy was introduced using the *d*-electron alloy design method with the aim of specific β phase stability beneficial to age-strengthening. For the newly designed alloy, the effect of aging temperature on microstructure and mechanical properties of Ti-6532 alloy has seldom been investigated so far. Thus, the microstructural evolution of this alloy during aging treatment was studied and the relationship between aging temperature, microstructures, strength and ductility was investigated as well.

1 Experiment

1.1 Alloy design

The *d*-electron method provides a physical background for the phase stability and phase transformation of titanium alloys by connecting the values of two parameters, *Bo* (covalent bond strength between Ti and alloying elements) and *Md* (mean orbital energy level concerned with electronegativity and elements radius). The average values of *Bo* and *Md* in titanium alloys are defined by $\overline{Bo}$ and $\overline{Md}$ as follows[16].

$$\overline{Bo} = \sum_{i}^{n} X_i (Bo)_i \quad (1)$$

$$\overline{Md} = \sum_{i}^{n} X_i (Md)_i \quad (2)$$

where X_i is the atomic fraction of the alloying elements in the alloy, $(Bo)_i$ and $(Md)_i$ are the corresponding values for the constituents. The Abdel-Hady's $\overline{Bo}$ - $\overline{Md}$ map shown in Fig.1 can be used as a semi-empirical tool to design new titanium alloys with specific phase stability and phase transformation. The main goal of designing this alloy is to achieve favorable mechanical properties, which can be improved by dispersed and fine α precipitates. Therefore, this is two-fold motivation. On the one hand, the β phase should be sufficiently stable so that almost all of metastable β phase can be retained to room temperature after quenching. On the other hand, the β phase should be sufficiently unstable so that precipitation of fine and dispersed α phase can be attained upon aging treatment. For this reason, the new alloy Ti-6Mo-5V-3Al-2Fe (wt%), named Ti-6532, was designed, in which part fraction of alloying element V was replaced by alloying element Mo according to commercial β titanium alloy Ti-1023. $\overline{Bo}$ value of the alloy is 2.776, while $\overline{Md}$ is 2.366. On the basis of $\overline{Bo}$ - $\overline{Md}$ map, the corresponding position of Ti-6532 alloy is located closely to the position of Ti-1023 alloy (Fig.1). Moreover, Ti-6532 alloy lies outside the martensite region but far away from the β titanium alloy region compared with Ti-1023 alloy. It can be predicted that the martensite cannot be formed after quenching and the low stability of β phase is inevitable.

The Mo equivalent ($[Mo]_{eq}$) is defined as the sum of the

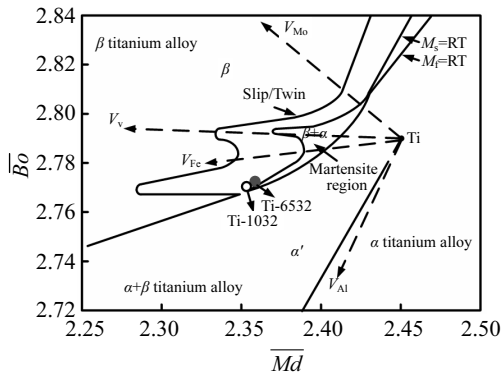

Fig.1 $\overline{Bo}$ - $\overline{Md}$ map and location of designed Ti-6532 alloy

averaged mass percent of alloying elements present in a titanium alloy and is used to quantify the stability of β phase in titanium alloys. The equation of $[Mo]_{eq}$ is given as follows[16].

$$[Mo]_{eq}=1.0Mo+0.67V+0.4W+0.28Nb+0.2Ta+1.25Cr+2.5Fe+1.7Mn+1.25Ni-1.0Al \quad (3)$$

According to Eq.3, the $[Mo]_{eq}$ of Ti-6532 alloy is 11.35, which is within the range of metastable β phase[17]. Because the $[Mo]_{eq}$ of Ti-6532 alloy is greater than that of Ti-1023 alloy, a higher stability of β phase can be obtained after quenching.

1.2 Material preparation

Sponge Ti, pure Mo, V-Al master alloy and V-Fe master alloy were used to prepare an ingot of the alloy. The raw materials were melted twice by a vacuum arc melting process to ensure chemical homogeneity. The chemical composition of the ingot determined by X-ray fluorescence spectroscopy is shown in Table 1.

The ingot with 120 mm in diameter and 200 mm in length was first forged into a plate with 100 mm in width and 30 mm in thickness. The plate was soaked in β field at 830 °C for 1 h and then multi-pass hot rolled at the same temperature into a plate with 6 mm in thickness followed by air cooling. The β-trans temperature of the alloy measured by metallographic method is 815±5 °C. The as-rolled specimens were solution treated at 850 °C for 0.5 h followed by water cooling. Then, the solution treated specimens were aged at 400, 450, 500, 550 and 600 °C, followed by air cooling. All specimens were aged for as long as 4 h to ensure sufficient precipitation of strengthening phase.

Two kinds of modified kroll's reagents (10 mL HF+30 mL HNO_3+50 mL H_2O and 10 mL HF+30 mL HNO_3+80 mL H_2O) were employed to reveal the microstructures of solution treated specimen and aging treated specimens, respectively.

Table 1 Chemical composition and Mo equivalent of as-designed alloy Ti-6532 (wt%)

Mo	V	Al	Fe	Ti
6.24	5.39	2.98	2.14	Bal.

The microstructures were characterized by optical microscope (OM, Zeiss AXIO Observer.A1m). Phase composition of solution treated specimen was identified by X-ray diffraction with Cu Kα radiation source. Discs with 500 μm in thickness were cut by electric sparking from the aged specimens. Then, the discs were manually ground to 50 μm and twin-jet thinned, and finally observed by transmission electron microscopy (TEM, JEOL Jem-2100) to observe precipitates. Effect of aging temperature on mechanical properties was evaluated by tensile test using MTS landmark 370.10 servo hydraulic test system. After tensile test, fracture surfaces were observed by scanning electron microscopy (SEM, Hitachi Su8010).

2 Results and Discussion

2.1 Microstructure characteristics of solution treated alloy

Microstructure of solution treated Ti-6532 alloy is shown in Fig.2a. The solution treatment mainly occurs in β field, so the metastable β phase can be retained to room temperature, while the β grains are rather coarse and the grain size is estimated to be ~210 μm. The XRD pattern of solution treated Ti-6532 alloy is shown in Fig.2b. Analyses of angles of X-ray diffraction peaks reconfirm that the solution treated alloy exhibits a single β phase structure. The main reason for such microstructure is that the β phase in Ti-6532 alloy has a high stability due to the higher $[Mo]_{eq}$, so it is stable enough to avoid the transformation of α phase and α' martensite during quenching. Without the formation of primary α phase and α' martensite, the β phase with relatively low concentration of β-stabilizer will be beneficial to precipitation of strengthening phase in the subsequent aging treatment.

2.2 Effect of aging temperature on microstructural evolution

To investigate the influence of aging temperature on the microstructural evolution of the Ti-6532 alloy, different aging temperatures from 400 °C to 600 °C were chosen. Microstructures of the specimen under various aging treatment conditions are compared in Fig.3. As shown in Fig.3, the

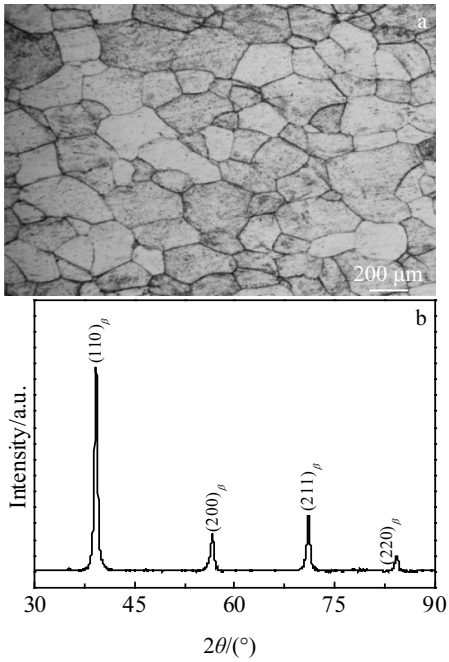

Fig.2 OM micrograph (a) and XRD pattern (b) of solution treated specimen

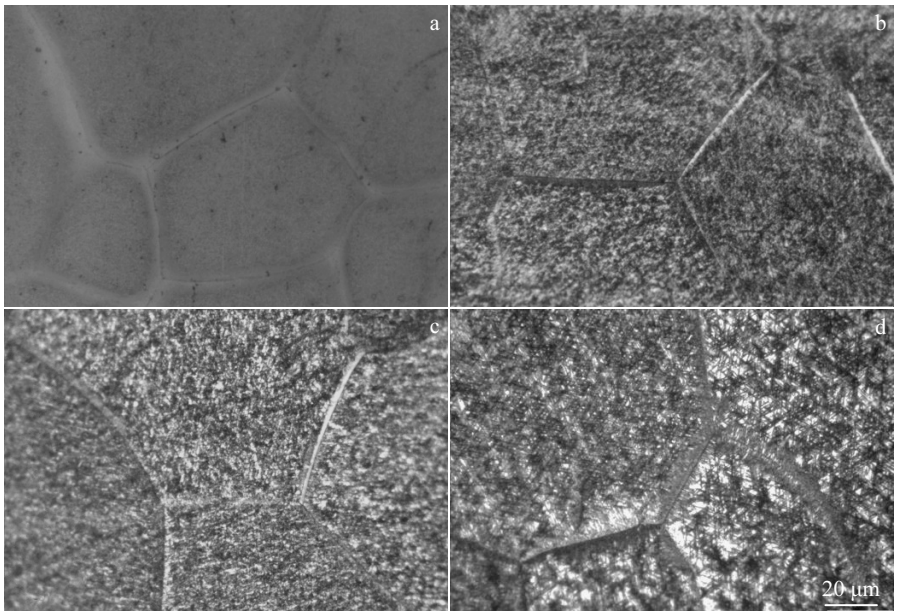

Fig.3 OM micrographs of specimens aging treated at 400 °C (a), 450 °C (b), 550 °C (c), and 600 °C (d)

secondary α phase within β grains can precipitate only at aging temperatures higher than 400 °C. This phenomenon indicates that low aging temperature of 400 °C cannot generate a high enough driving force for the nucleation of secondary α phase. When the aging temperature is higher than 400 °C, the bulk secondary α precipitates within β grains can be observed (Fig.3b~3d). However, Fig.3b and Fig.3c reveal only the minor differences in microstructure of alloys aged at 450~550 °C, since the secondary α phase are too fine to be identified in OM micrographs. Furthermore, another microstructural feature in these specimens aged at 450, 500 and 550 °C has been found. As seen from Fig.3b and 3c, a narrow white area surrounded by the secondary α precipitates is clearly visible near the β grain boundaries. The similar microstructure feature of aged specimen of commercial metastable β titanium alloy β-CEZ has been reported by previous research, and the narrow white zone has been confirmed as a precipitate free zone (PFZ)[18]. The possible reason for the formation of PFZ is the limited diffusion distance of the alloying elements during the phase transformation[18]. The grain boundary α (α_{GB}) nucleated and grown preferentially due to supply of nucleation sites by grain boundaries has a large amount of defects, and the β-stabilizer, such as Mo, V and Fe, diffuses to the vicinity of β phase. As a result, it is hard to precipitate secondary α phase in such a chemically stable zone with enrichment of β-stabilizer. However, when aging temperature is 600 °C, the PFZ disappears and the amount of precipitates within β grains decreases (Fig.3d).

Further observations of precipitates were carried out on TEM. Fig.4 shows TEM micrographs of specimens aged at various temperatures, in which acicular secondary α phases are precipitated within the β grains. When the aging temperature is 450 °C, the acicular α precipitates are quite refined, and the average width is ~49 nm. It is postulated that the main reason for the precipitation of such fine α phase is some kinds of precursors forming before aging treatment, and accelerating the nucleation rate of α phase. In general, these precursors can be dislocations or metastable ω particles. Since the alloy undergoes thermal deformation at β field before aging treatment, the dynamic recovery and dynamic recrystallization induce the dislocation annihilation. However, for the β titanium alloy with $[Mo]_{eq}$ of ~11, the metastable ω phase can form spontaneously during quenching through an athermal and displacive mechanism[19]. The formation of ω phase in β-CEZ alloy that is located closely to the position of Ti-6532 alloy in $\overline{Bo}$ - $\overline{Md}$ map has been reported by previous researches[20]. Therefore, it can be proposed that the metastable ω phase may be formed before aging treatment and acts as a precursor for fine α precipitates in Ti-6532 alloy. However, the ω phase was not detected in XRD pattern of solution treated specimen (Fig.2b). And this may be attributed to the fact that the size of ω phase is too fine or the volume fraction of ω phase is too small to be detected by XRD. Previous literatures reported that ω phase can stimulate the nucleation of α phase and promote the uniform distribution[21]. During aging treatment at 450 °C, the ω phase provides nucleation sites for α phase, resulting in fine and dispersed precipitation.

According to Fig.4b, the increase of aging temperature results in a growth of α precipitates. It is worth noting that the coarse secondary α phase with an average width of ~290 nm precipitates in the alloy aged at 600 °C. With the growth of α phase, the inter-particle spacing of α phase becomes broad. The reason behind the change in inter-particle spacing is that the precipitation of α phase results in a β-stabilizer-rich zone near the precipitators, and the bigger α precipitates give rise to a broader precipitate free zone that has a greater inter-particle spacing of α phase.

TEM micrograph near β grain boundary in the specimen aged at 600 °C is shown in Fig.5. The β grain boundaries are decorated by continuous α_{GB}. Besides the continuous α_{GB}, secondary α phase precipitates on α_{GB} and forms a parallel colony that can be observed as Widmanstätten laths near prior β grain boundaries (hereafter called α_{WGB}). The similar formation of such secondary α laths has been reported [22]. A high aging temperature will accelerate the diffusion of β-stabilizer, resulting in a decrease of stability of PFZ near the β grain boundaries. So the precipitation of α_{WGB} can get a higher driving force at the aging temperature of 600 °C, then resulting in the formation of α_{WGB} crossed the PFZ.

Based on our recent works, a schematic illustration shown in Fig.6 is proposed to reveal the precipitation mechanism of secondary α phase affected by aging temperature in Ti-6532 alloy. The α_{GB} and acicular α phase nucleate preferentially at

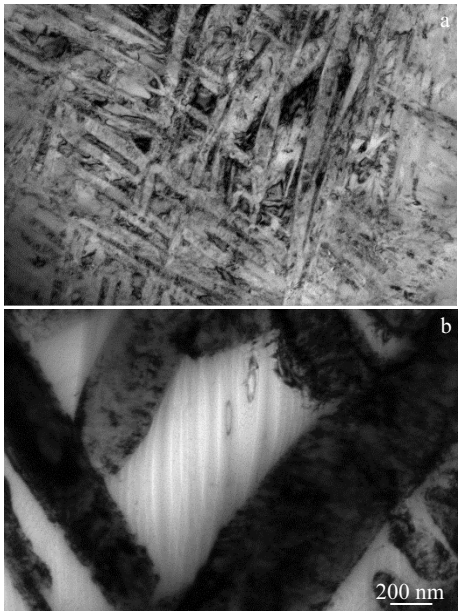

Fig.4 TEM images of alloys aged at 450 °C (a) and 600 °C (b)

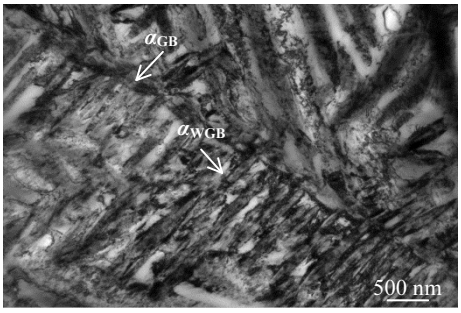

Fig.5 TEM image of the microstructure near β grain boundaries of alloys aged at 600 °C

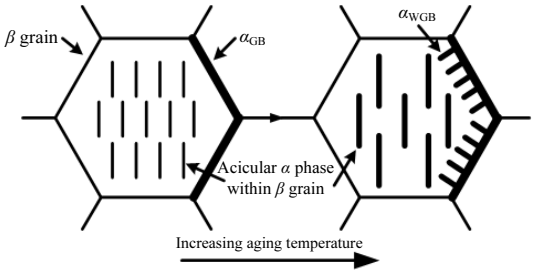

Fig.6 Schematic illustration of precipitation mechanism of secondary α phase affected by aging temperature

prior grain boundaries and within β grains, respectively. With the increase of aging temperature, in addition to increasing the size and inter-particle spacing of acicular secondary α phase within β grains, the α_{WGB} nucleates and grows into β grains. When α_{WGB} grows cross the PFZ, the coarse α phase within β grains can prevent the further growth of α_{WGB}.

2.3 Effect of aging temperature on mechanical properties

The curves in Fig.7 show tensile properties of alloys aged at various temperatures. As can be seen from the curves, when the aging temperature is higher than 400 °C, the strength of the alloy is improved significantly. This phenomenon indicates that the precipitation of secondary α phase within β grains is the main reason for the improvement of alloy strength. As the aging temperature increases to 450 °C, the strength of the alloy reaches the peak value of yield strength (YS) of 1395 MPa and ultimate tensile strength (UTS) of 1510 MPa, while the elongation (EL) reaches the lowest value of 4.6%. Under such an aging condition, the alloy with the finest secondary α precipitates within β grains obtains the highest strength but the lowest elongation. This means that the mechanical properties of the alloy are very sensitive to the microstructural characterization, especially to the morphology of secondary α phase. When the aging temperature is higher than 500 °C, the strength decreases with increasing the aging temperature, but the ductility changes in an opposite way. Particularly, as the aging temperature increases to 600 °C, the alloy has the greatest

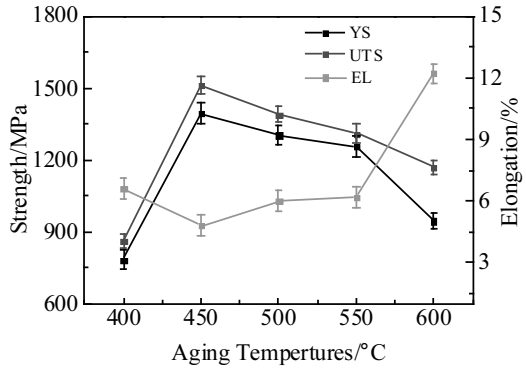

Fig.7 Tensile properties of the specimens aged at various temperatures

elongation (12.2%) and acceptable UTS (1170 MPa).

Generally speaking, alloy strength is mainly determined by size, quantity and morphology of α phase[23]. The more amount and smaller size of the acicular secondary α phase within the β matrix will provide more α/β interfaces, which can act as effective dislocation barriers[24]. The influence of α phase on the yield strength of the β titanium alloy can be expressed by the following equation[19].

$$\sigma_y = \frac{K_p}{l_p} + \frac{K_s}{l_s} \tag{4}$$

where σ_y is yield strength of β titanium alloy, l_p is inter-particle spacing of primary α phase, l_s is inter-particle spacing of secondary α phase, and K_p and K_s are constants including the Taylor factor. As indicated in Eq.(4), the alloy strength decreases with the increase of inter-particle spacing of secondary α phase. The bigger secondary α phase leads to a greater value of l_s, thus resulting in a decrease in the strength. Therefore, the alloy aged at 500 °C exhibits the highest strength due to the finest secondary α phase and the smallest inter-particle spacing of secondary α phase.

It can be speculated that the poor ductility of specimen aged at 450 °C is mainly attributed to the negative effect of preferentially formed α_{GB} on the alloy ductility. Because of the different crystal structures, α_{GB} and β phase have different strengths. In addition, when aged at 450 °C, due to the formation of PFZ, the continuous α_{GB} is even softer compared with the age-hardened β matrix[23]. During the tensile test, the crack propagation leads to an intergranular fracture along the β grain boundaries. Such speculation can be confirmed by the fracture of tensile specimen. The fractures of the tensile specimens aged at 450 and 600 °C are shown in Fig.8. As shown in Fig.8a, when the alloy aged at 450 °C has the lowest elongation of 4.6%, the fracture shows intergranular (rock candy pattern) and transgranular (crystal cleavage) failure. The failure indicates that the crack can always propagate along the grain boundaries. Such fracture morphology also demonstrates that the alloy has a poor ductility.

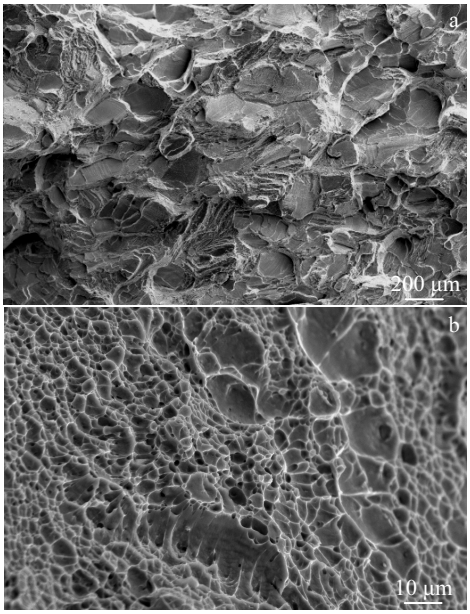

Fig.8 SEM images of the fracture morphology of the specimens aged at 450 °C (a) and 600 °C (b)

With the increase of aging temperature above 500 °C, the strength decreases and the ductility changes in an opposite way. This trend also occurs in other β titanium alloys such as Ti-3.5Al-5Mo-6V-3Cr-2Sn-0.5Fe[25]. According to Fig.5, α_{WGB} can form when aged at a higher temperature of 600 °C. For the specimen with α_{WGB}, the crack occurs not only at α_{GB}/β interface but also at α_{WGB}/β interface. Therefore, the α_{WGB} can deflect the crack propagation direction, resulting in the improvement of alloy ductility. In addition, the broad inter-particle spacing of secondary α phase within β grains increases the slip distance for dislocation movement. As a result, for the specimen aged at 600 °C, a significant improvement of ductility can be obtained. As shown in Fig.8b, the fracture surface of specimen aged at 600 °C consists mainly of large amounts of dimples. Fracture morphology analyses show that the fracture changes from a brittle fracture to a ductile fracture. Such fracture morphology proves that the alloy ductility is improved.

3 Conclusions

1) A novel β titanium alloy Ti-6Mo-5V-3Al-2Fe (wt%, Ti-6532) is designed according to *d*-electron alloy design method. The β phase of the as-designed Ti-6532 alloy is stable enough to avoid the transformation of α phase and α' martensite after quenching, whereas is sufficiently unstable so that the precipitation of fine and dispersed α phase can occur during aging treatment.

2) Ultimate tensile strength of 1510 MPa has been obtained when aging at 450 °C, due to the formation of acicular secondary α phase within β grains with the small size of ~49 nm. The increase of aging temperature leads to the increase in size and inter-particle spacing of secondary α phase within β grains, resulting in the decrease of strength.

3) Under the synergic influences of the formation of parallel secondary α laths near β grain boundaries and the broad inter-particle spacing of secondary α phase within β grains, the ductility can be improved significantly. The alloy can achieve the improvement of elongation to 12.2% and acceptable ultimate tensile strength of 1170 MPa after aged at 600 °C.

References

1 Brozek C, Sun F, Vermaut P *et al*. *Scripta Materialia*[J], 2016, 114: 60
2 Hou Z M, Zhao Y Q, Zeng W D *et al*. *Rare Metal Materials and Engineering*[J], 2017, 46(8): 2087
3 Fan X G, Zhang Y, Gao P F *et al*. *Materials Science and Engineering A*[J], 2017, 694: 24
4 Ji X, Emura S, Min X H *et al*. *Materials Science and Engineering A*[J], 2017, 702: 701
5 Zhou W, Ge P, Zhao Y *et al*. *Rare Metal Materials and Engineering*[J], 2017, 46(10): 2852
6 Chao L, Zhang X Y, Li Z Y *et al*. *Rare Metal Materials and Engineering*[J], 2015, 44(2): 327
7 Min X H, Chen X J, Emura S *et al*. *Scripta Materialia*[J], 2013, 69(5): 393
8 Sun F, Zhang J Y, Marteleur M *et al*. *Scripta Materialia*[J], 2015, 94: 17
9 Zhang J Y, Li J S, Chen Z *et al*. *Journal of Alloys and Compounds*[J], 2017, 699: 775
10 Lee S W, Park C H, Hong J K *et al*. *Materials Science and Engineering A*[J], 2017, 697: 158
11 Shekhar S, Sarkar R, Kar S K *et al*. *Materials and Design*[J], 2015, 66: 596
12 Du Z X, Xiao S L, Xu L J *et al*. *Materials and Design*[J], 2014, 55: 183
13 Li C L, Zou L N, Fu Y Y *et al*. *Materials Science and Engineering A*[J], 2014, 616: 207
14 Abdel-Hady M, Hinoshita K, Morinaga M. *Scripta Materialia*[J], 2006, 55(5): 477
15 Liang S X, Feng X J, Yin L X *et al*. *Materials Science and Engineering C*[J], 2016, 61: 338
16 Sadeghpour S, Abbasi S M, Morakabati M. *Journal of Alloys and Compounds*[J], 2015, 650: 22
17 Nyakana S L, Fanning J C, Boyer R R. *Journal of Materials Engineering and Performance*[J], 2015, 14(6): 799
18 Li C, Chen J, Li W *et al*. *Journal of Alloys and Compounds*[J], 2016, 684: 466
19 Ren L, Xiao W L, Chang H *et al*. *Materials Science and Engineering A*[J], 2018, 711: 553
20 He T, Feng Y, Luo W Z *et al*. *Materials Characterization*[J], 2018, 138: 19

21 Ng H P, Devaraj A, Nag S *et al. Acta Materialia*[J], 2011, 59(8): 2981
22 Wang K, Li M Q. *Materials Science and Engineering A*[J], 2014, 613: 209
23 Huang L G, Chen Y Y. *Journal of Alloys and Compounds*[J], 2015, 646: 557
24 Du Z X, Xiao S L, Shen Y P *et al*. *Materials Science and Engineering A*[J], 2015, 631: 67
25 Chen Y Y, Du Z X, Xiao S L *et al*. *Journal of Alloys and Compounds*[J], 2014, 586: 588

时效温度对一种新型 β 钛合金组织演变及力学性能的影响

张浩宇[1,2]，黎小辉[1]，林　立[2]，张思倩[2]，王　川[3]，陈立佳[2]

(1. 广东省金属强韧化技术与应用重点实验室，广东 广州 510650)

(2. 沈阳工业大学，辽宁 沈阳 110870)

(3. 沈阳航天新光集团，辽宁 沈阳 110861)

摘　要：采用 *d*-电子合金设计法设计了一种 β 钛合金，Ti-6Mo-5V-3Al-2Fe（质量分数）。在 450~600 ℃范围内选取了多个时效温度进行时效处理，以研究时效温度对该合金组织演变及力学性能的影响。结果表明，当时效温度为 500 ℃时，在 ω 辅助形核机制作用下，形成了尺寸和相间距更小的次生 α 相，在此细小的次生 α 相对 β 基体的强化作用下合金抗拉强度达到最大值 1510 MPa；同时，由于晶界 α 相的析出以及晶界无析出区的形成，导致合金的塑性极差，伸长率仅为 4.6%。随着时效温度的升高，晶内细小的次生 α 相粗化。粗大的次生 α 相导致其相间距增大，并使可有效阻碍位错运动的 α/β 相界面减小。时效温度的升高使合金强度降低，但合金塑性提高。当时效温度升高至 600 ℃，在 β 晶界处形成了向晶内平行生长的板条状次生 α 相，同时 β 晶粒内次生 α 相间距增大，使合金塑性明显提高，伸长率可达 12.2%。

关键词：β 钛合金；时效处理；次生 α 相；显微组织；力学性能

作者简介：张浩宇，男，1987 年生，博士，讲师，沈阳工业大学材料科学与工程学院，辽宁 沈阳 110870，电话：024-25494501，E-mail: zhanghaoyu@sut.edu.cn